

Room Temperature Electrical Detection of Spin Coherence in C₆₀

W. Harneit,^{1,2,*} C. Boehme,^{3,4,†} S. Schaefer,¹ K. Huebener,^{1,2} K. Fostiropoulos,² and K. Lips⁴

¹*Institut für Experimentalphysik, Freie Universität Berlin, Arnimalle 14, 14195 Berlin, Germany*

²*Abteilung Heterogene Materialsysteme, Hahn-Meitner-Institut Berlin, Glienicker Strasse 100, 14109 Berlin, Germany*

³*Department of Physics, University of Utah, 115 S 1400 E, Suite 201, Salt Lake City, Utah 84112-0830, USA*

⁴*Abteilung Silizium-Photovoltaik, Hahn-Meitner-Institut Berlin, Kekuléstrasse 5, 12489 Berlin, Germany*

(Received 23 February 2007; published 21 May 2007)

An experimental demonstration of electrical detection of coherent spin motion of weakly coupled, localized electron spins in thin fullerene C₆₀ films at room temperature is presented. Pulsed electrically detected magnetic resonance experiments on vertical photocurrents through Al/C₆₀/ZnO samples showed that an electron spin Rabi oscillation is reflected by transient current changes. The nature of possible microscopic mechanisms responsible for this spin to charge conversion as well as its implications for the readout of endohedral fullerene (N@C₆₀) spin qubits are discussed.

DOI: [10.1103/PhysRevLett.98.216601](https://doi.org/10.1103/PhysRevLett.98.216601)

PACS numbers: 72.80.Le, 03.67.Lx, 76.30.-v, 85.75.-d

The need for very sensitive spin measurement techniques for small electron ensembles, possibly even single spins, in organic semiconductors has grown significantly in recent years, because of the following. (i) The development of organic spintronic devices has progressed and the possibility of spin injection [1], spin transport [2], and spin valves [3,4] is increasingly investigated. (ii) Coherent spin measurements have become important for the investigation of spin-dependent processes in organic devices under operating conditions (room temperature). Examples are singlet-triplet mixing mechanisms in organic light emitting diodes [5] or spin-dependent recombination in organic solar cells, which are both relevant in order to assess the true energy efficiency limitations of these devices. (iii) Organic molecular systems such as endohedral fullerenes exhibit extremely long spin coherence times at room temperature [6] suggesting a possible use for room temperature quantum information applications [6–9].

Traditional electron spin measurement techniques such as electron paramagnetic resonance (EPR) lack the sensitivity required for the minute number of spins present in the low dimensional geometries of many organic semiconductor devices. Several experimental demonstrations of much more sensitive measurement approaches based on electrical spin detection using spin to charge conversion mechanisms have been reported for various electronic or nuclear spin systems such as localized point defects of inorganic semiconductors [10–13] or semiconductor quantum dots [14,15]. Most of these approaches are confined to low temperatures ($T \leq 5$ K), in part due to the short coherence times of the comparatively strongly spin-orbit-coupled spins in inorganic semiconductors at higher temperatures. In contrast, organic semiconductors are known to possess paramagnetic centers with extraordinarily long coherence times at higher temperatures and even at room temperature [6]. However, to our knowledge, there have been no reports of experimental demonstrations for coherent electrical spin detection in organic semiconductors thus far.

In the following, we report on the experimental demonstration of coherent spin measurements of localized paramagnetic states in fullerene C₆₀ layers at room temperature by purely electrical means, namely, through transient measurements of electric currents that are governed by spin-selection rules. To this end, pulsed electrically detected magnetic resonance (pEDMR) experiments were conducted on vertical photocurrents through thin C₆₀ films in transient nutation style experiments [13].

Several samples were prepared for this study, with 80–300 nm thick fullerene films sandwiched between two Al electrodes, or between Al and ZnO. The influence of these variations on the results is minor and will be addressed elsewhere. All layers were evaporated in ultrahigh vacuum and the samples were encapsulated in quartz tubes in an inert-gas glove box without intermediate exposure to air that could negatively affect the electronic properties of the thin films. The active device area was 2 mm × 2 mm and thin contact stripes were extended on a 2.6 mm × 58 mm substrate towards a region outside the resonator, in order to minimize field mode distortions in the resonator. The pEDMR measurements were carried out on a commercial pulsed ESR X-band spectrometer (Bruker E580). The sample was illuminated through the optical view port of the resonator and through one of the contact layers with a halogen lamp (110 W) and an argon ion laser (488 nm, up to 1 W power). The photoinduced bias current I_0 was stabilized by a current source with a long time constant, so that the transient current response (extending to ≈ 100 μ s) after the microwave pulses was not averaged out. The amplitude B_1 of the microwave field was calibrated using a 4-hydroxy-2,2,6,6-tetramethylpiperidine-*N*-oxyl (Tempol) standard (Sigma Aldrich).

Figure 1 shows the transient current response ΔI to microwave pulses as a function of time t [1(a)] and magnetic field B_0 [1(c)]. The 2D data set [1(b)] was modeled with a global 2D fit [1(d)]. The fit function $\Delta I(t, B_0) = I_{\text{ph}}(t)\Delta(B_0)$ is a product function of the time evolution of

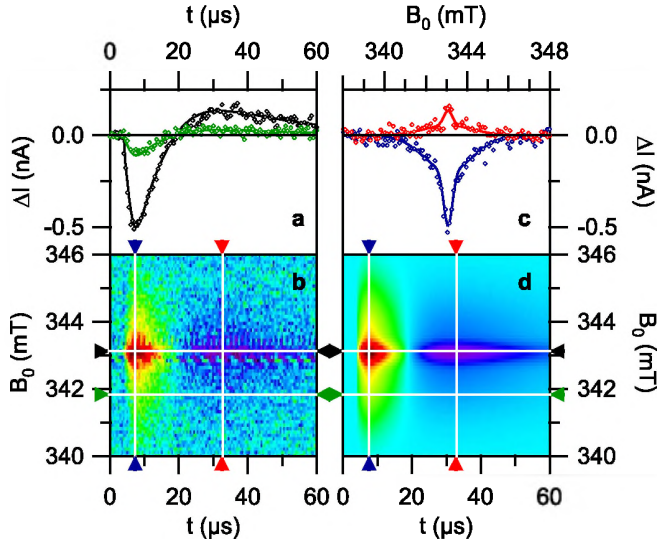


FIG. 1 (color online). Transient current ΔI of a $N@C_{60}$ film illuminated with a halogen lamp ($\approx 10 \text{ mW/cm}^2$, $I_0 = 10 \mu\text{A}$) after 320 ns long microwave pulses ($B_1 \approx 63 \mu\text{T}$). Time traces (a) were recorded at different magnetic fields B_0 to afford the 2D data set (b). 1D cuts along the field dimension (c) reveal the spectral behavior. (d) Displays a global fit of the data in (b) together with an indication where the cuts (a),(c) were taken; in these, the data are represented by markers, whereas the global fit is drawn as lines.

the current

$$I_{\text{ph}}(t) = (1 - e^{-(t/t_s)}) \sum_{j=1, \dots, 3} I_j e^{-(t-t_d)/\tau_j} \quad (1)$$

and the spectroscopic function

$$\Delta(B_0) = \frac{2}{\pi} \sum_k \frac{\Delta B_k}{4(B_0 - \frac{h\nu_0}{\mu_B} g_k^{-1})^2 + \Delta B_k^2}, \quad (2)$$

which is a multiple Lorentzian normalized to unit area containing Planck's constant h , Bohr's magneton μ_B , the microwave frequency ν_0 , and the Landé factor g_k and full width at half height ΔB_k for each resonance line k . The time evolution is described by the signed weights I_j and time constants τ_j of the multiexponential decay expected from theory [[16], Eq. (25)], a pulse trigger delay t_d , and a saturation time t_s describing the response of the detection circuit which is due to a finite rise time.

Because of the product decomposition of $\Delta I(t, B_0)$, the spectroscopic information can be interpreted independently of the time evolution of the current if the latter is integrated out. The resulting charge-equivalent pEDMR signal $Q(B_0) = \int \Delta I(t, B_0) dt$ contains all spectroscopic information. In general, the integration limits are chosen to give maximal Q and the integration can be carried out using the hardware of the ESR spectrometer. Careful analysis reveals that the spectroscopic information contained in $Q(B_0)$ does not depend on that choice. The magnitude of Q is a direct measure of the number of

carriers involved in the spin-dependent process. It turns out that our room temperature pEDMR signal is due to $\approx (1-2) \times 10^4$ elementary charges. In this small-ensemble regime, an exact model of the charge carrier dynamics is needed in order to relate the number of charges to the number of spins since the constants I_j and τ_j depend in general on numerous parameters such as capture and emission cross sections of traps as well as carrier generation and recombination rates. Even in the best of cases, these parameters are hard to deconvolve quantitatively [17], and we do not attempt this in this Letter. The spectroscopic information obtained from the data of Fig. 1 and similar data (not shown here) can be summarized as follows. (i) The signal is observed on some, but not on all samples prepared. (ii) It is observed only under illumination, and consistently absent in the dark. (iii) The initial sign of the signal is negative, corresponding to current quenching while at times $t \geq 20 \mu\text{s}$ the sign reverses to current enhancement. (iv) The signal magnitude $|\Delta I|$ depends on the samples investigated (by a factor of 2 at least), but (v) $|\Delta I|$ depends only weakly on the illumination intensity or wavelength. (vi) The resonance condition is fulfilled at $g = 2.0018(5)$, and (vii) the smallest observed linewidth is $\Delta B_a \leq 0.3 \text{ mT}$. (viii) Measurements at low amplitude $B_1 < 0.2 \text{ mT}$ show a second, much broader line ($\Delta B_b \approx 3 \text{ mT}$) at the same g factor within our resolution.

Figure 2 shows the evolution of Q as a function of microwave pulse length τ for three different microwave amplitudes B_1 . The observed oscillatory behavior is due to transient nutation of the spin pair state. The coherent pulses induce Rabi oscillations of angular frequency $\omega_R = 2\kappa\omega_1 = 2\kappa\gamma B_1$, where $\gamma = g\mu_B/h$ is the gyromagnetic ratio. The Rabi frequency ω_R is indicative of the spin quantum number S via the factor κ [16], expected to be $\kappa = 1/2$ for resonance of only one of the two weakly coupled $S = \frac{1}{2}$ spins ("doublet"), $\kappa = \sqrt{1/2}$ for a strongly coupled pair with $S = 1$ ("triplet"), and $\kappa = 1$ for a pair of coupled $S = \frac{1}{2}$ spins when their spectroscopic separation is small: $\hbar\Delta\omega_L \equiv |g_1 - g_2|\mu_B B_0 \ll \hbar\omega_1$, J where J is the effective spin-spin coupling constant. As demonstrated in Fig. 2(a) by the comparison of the data to the "transient function" $T(\alpha)$ with $\alpha = \kappa\gamma B_1 \tau$ [16], we observe a Rabi frequency $\omega_R = \omega_1 = \gamma B_1$, as expected for $S = \frac{1}{2}$. It can easily be shown that $T(\alpha)$ is related to the Bessel function of the first kind J_0 ,

$$T(\alpha) = \pi \int_0^\alpha J_0(2x) dx. \quad (3)$$

For large arguments ($\alpha > \pi/2$), $T(\alpha)$ is a quasiperiodic function of the nutation or "turning" angle $2\alpha = \omega_R \tau$ resembling a damped sinusoid. This "built-in" damping is due to the fact that selective excitation of an inhomogeneously broadened line was assumed for the derivation of $T(\alpha)$ and is not indicative of spin relaxation in itself, it reflects a coherent dephasing process amenable to refocusing techniques [18]. Figure 2(b) shows the fast Fourier

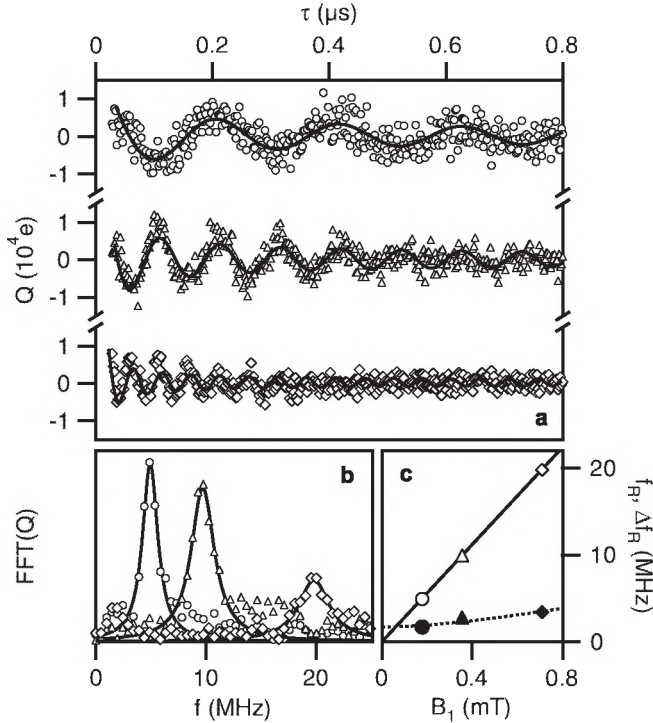


FIG. 2. (a) Oscillatory part of the observable Q as a function of microwave pulse length at different pulse amplitudes B_1 for a C_{60} film illuminated with an argon ion laser (< 100 mW/cm 2 , $I_0 = 50$ μ A). The lines are fits using the theoretical curve $T(\alpha = \kappa \gamma B_1 \tau)$ given in Eq. (3). (b) Fast Fourier transforms of the data in (a) and Lorentzian fits. (c) Rabi frequencies f_R (open symbols) and resonance widths Δf_R (solid symbols) extracted from the fits in (b). The full line in (c) is $f_R = \gamma B_1 / 2\pi$, the expected behavior of a spin $S = \frac{1}{2}$. The dotted line is the prediction of the linewidth as a function of B_1 based on the assumption of a $\approx 15\%$ field inhomogeneity.

transform (FFT) of the data displayed in Fig. 2(a), together with Lorentzian fits. *a priori*, the width of the Lorentzian Δf_R should not depend on the microwave field strength B_1 . The observed slight increase in width, reported together with the Rabi frequency in Fig. 2(c), may be due to an inhomogeneity in the B_1 microwave field. In a simple model, the detected FFT width can be described by $\Delta f_R^2 = \Delta f_{\text{int}}^2 + (\Delta \omega_1 / 2\pi)^2$, where $\Delta f_{\text{int}} \approx 1.7$ MHz is due to the built-in damping and a relative B_1 field inhomogeneity which turns out to be $\Delta \omega_1 / \omega_1 \approx 15\%$ for the data presented in Fig. 2(c). To summarize the coherent properties at room temperature, Rabi oscillation experiments similar to those reported in Fig. 2 reveal (i) a B_1 dependence of the Rabi frequency consistent with $S = \frac{1}{2}$ character of the signal, (ii) a damping behavior consistent with an inhomogeneously broadened “partner line,” which is visible in the spectra only at low B_1 amplitudes, and (iii) coherent oscillations with a damping time $\Delta f_{\text{int}}^{-1} \approx 0.6$ μ s, which is limited by the inhomogeneity of the spin ensemble and not by the intrinsic T_2 decoherence time. An estimate for T_2 may be obtained using Rabi echoes and other refocusing techniques [18].

The experimental data presented in Figs. 1 and 2 show that the magnetic resonant current imprint of the paramagnetic centers with Landé factor around $g \approx 2.0018(5)$ and with weakly coupled ($S = \frac{1}{2}$) systems can be observed by means of transient measurements of the photocurrent changes after coherent spin excitations at room temperature. The magnetic field spectra of the current response suggest that two different resonances are present with linewidths of ≈ 3 and ≈ 0.3 mT, respectively. With the given accuracies, an undisputable association of the Landé factors with particular spin systems is difficult since various paramagnetic states in C_{60} are known [19–21], such as the corresponding fullerene radical states and other impurity states, as they may occur in the used device system. With the given experimental data, it is possible that the current is governed by spin-dependent recombination of excess charge carriers similar to the model described for inorganic semiconductors [16] assuming that the observed spins are due to localized defect levels which enhance recombination. It is also possible that the currents are controlled by polaron pair quenching upon polaron pair encounter with radicals. The latter has been referred to as the radical-triplet pair mechanism in the literature [22]. Thus, while the experimental data presented here cannot conclusively rule out any of these different explanations for the observed signals, there is strong evidence for a spin-dependent recombination mechanism of weakly coupled spin pairs ubiquitous in fullerenes [19] since (i) the nature and spectroscopic properties of these pairs are in accordance with the two observed resonances, (ii) the mechanism requires the detection of spin $S = \frac{1}{2}$ pair partners which have been confirmed by the data, and (iii) the theoretically well investigated dynamical nature of such pairs after coherent spin excitations [7,16,23] is entirely consistent with the current transients observed here. The well understood current quenching followed by current enhancement is characteristic for such mechanisms: It is due to the electronic relaxation of first singlet and then triplet pair densities. In spite of this strong agreement, we want to point out nevertheless that, in the absence of theoretical predictions for pEDMR transients due to the other spin-dependent mechanisms described in the literature, the microscopic nature of the observed signals cannot be verified with certainty.

The process responsible for the signals discussed above represents a spin to charge conversion for weakly coupled, localized spin states in a C_{60} solid at room temperature. We believe that this finding may have important implications for the development of highly sensitive spin quantum read-out schemes for endohedral fullerene ($N@C_{60}$) based electron spin qubits [6]. For spin-dependent recombination through weakly coupled spin pairs as assumed above, an identification of the integrated current (corresponding to the number of detected charge carriers and therefore the number of detected spin-dependent transitions) with the number of paramagnetic centers involved in these transi-

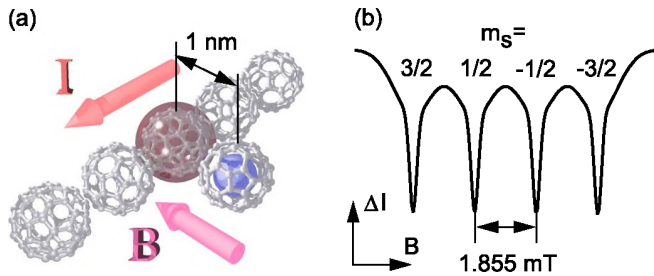


FIG. 3 (color online). (a) Schematic illustration of an electrical readout of a $N@C_{60}$ endohedral fullerene spin. The localized spin involved in spin-dependent transitions, marked by a surrounding sphere, is dipolarly coupled to the adjacent $N@C_{60}$ spin. (b) The expected spectrum for 52 MHz strong coupling of the $S = \frac{3}{2}$ $N@C_{60}$ spin to an $S = \frac{1}{2}$ state in C_{60} .

tions is possible [16]. Hence, for the macroscopic samples used in this study, a sensitivity of $\approx 10^4$ spins is given. This is many orders of magnitude more sensitive than conventional EPR measurements on C_{60} and endohedral $N@C_{60}$ molecules. Note that the given sensitivity limitations were caused by shot noise due to spin-independent shunt currents. It is conceivable that the same signals reach even higher sensitivities by improved sample designs oppressing these shunt currents. Thus, we believe the spin to charge conversion mechanism observed here may be suitable for a dipolar coupling mediated readout of electron spins of endohedral fullerenes as illustrated in Fig. 3. Here, the localized paramagnetic state whose spin governs charge carrier recombination is represented by a closed sphere due to its unknown nature. If this probe spin is in spatial proximity to an $N@C_{60}$ qubit molecule, the state of the probe spin will be shifted by the four eigenstates of the $S = \frac{3}{2}$ qubit. For the case of maximal dipolar coupling (reached at an angle $\theta = 0$ between the qubit-probe spin axis and the direction of an applied magnetic field) and an assumed distance of $r = 1$ nm, a splitting of the probe spin resonance into four lines with 1.855 mT separation can be expected. Hence, if we assume a line width of 0.3 mT (see Fig. 1) for the electrically read probe spin, the given line separation should be sufficient for a distinction of the qubit eigenstates required for a readout.

In conclusion, we report on a very sensitive electrical detection of coherent spin motion of localized, weakly coupled electron spins in thin C_{60} films at room temperature which has been demonstrated by means of transient photocurrent measurements after short coherent electron spin resonant excitation. The observed data reveal the presence of electron spin Rabi oscillation of paramagnetic centers at a Landé factor of $g \approx 2.0018(5)$. The nature of the observed signals is in agreement with described spin-dependent charge carrier pair recombination models. It has been pointed out that the ability to coherently measure (read) localized electron spin states in C_{60} solids with high sensitivity may be utilized as a potential readout mechanism for endohedral $N@C_{60}$ fullerene qubits.

We thank Jan Behrends (Hahn-Meitner-Institut) for support in the pEDMR measurements and Carola Meyer (Forschungszentrum Jülich) for helpful discussions. This work was funded in part by the Bundesministerium für Bildung und Forschung (Contract No. 03N8709).

*Corresponding author.

Electronic address: harneit@physik.fu-berlin.de

*Corresponding author.

Electronic address: boehme@physics.utah.edu

- [1] V. Dediu, M. Murgia, F.C. Maticcotta, C. Taliani, and S. Barbanera, *Solid State Commun.* **122**, 181 (2002).
- [2] K. Tsukagoshi, B.W. Alphenaar, and H. Ago, *Nature (London)* **401**, 572 (1999).
- [3] Z.H. Xiong, D. Wu, Z. V. Vardeny, and J. Shi, *Nature (London)* **427**, 821 (2004).
- [4] J.R. Petta, S.K. Slater, and D.C. Ralph, *Phys. Rev. Lett.* **93**, 136601 (2004).
- [5] S.R. Forrest, *Nature (London)* **428**, 911 (2004).
- [6] W. Harneit, *Phys. Rev. A* **65**, 032322 (2002).
- [7] M. Mehring, W. Scherer, and A. Weidinger, *Phys. Rev. Lett.* **93**, 206603 (2004).
- [8] J.J.L. Morton, A.M. Tyryshkin, A. Ardavan, K. Porfyakis, S.A. Lyon, and G. Andrew D. Briggs, *Phys. Rev. Lett.* **95**, 200501 (2005).
- [9] J.J.L. Morton, A.M. Tyryshkin, A. Ardavan, S.C. Benjamin, K. Porfyakis, S.A. Lyon, and G. Andrew D. Briggs, *Nature Phys.* **2**, 40 (2006).
- [10] C. Boehme and K. Lips, *Phys. Rev. Lett.* **91**, 246603 (2003).
- [11] M. Xiao, I. Martin, E. Yablonovitch, and H.W. Jiang, *Nature (London)* **430**, 435 (2004).
- [12] A.D. Greentree, A.R. Hamilton, L.C.L. Hollenberg, and R.G. Clark, *Phys. Rev. B* **71**, 113310 (2005).
- [13] A.R. Stegner, C. Boehme, H. Huebl, M. Stutzmann, K. Lips, and M.S. Brandt, *Nature Phys.* **2**, 835 (2006).
- [14] J.R. Petta, A.C. Johnson, J.M. Taylor, E.A. Laird, A. Yacoby, M.D. Lukin, C.M. Marcus, M.P. Hanson, and A.C. Gossard, *Science* **309**, 2180 (2005).
- [15] F.H.L. Koppens, C. Buizert, K.J. Tielrooij, I.T. Vink, K.C. Nowack, T. Meunier, L.P. Kouwenhoven, and L.M.K. Vandersypen, *Nature (London)* **442**, 766 (2006).
- [16] C. Boehme and K. Lips, *Phys. Rev. B* **68**, 245105 (2003).
- [17] C. Boehme and K. Lips, *Phys. Status Solidi C* **1**, 1255 (2004).
- [18] S. Stoll, G. Jeschke, M. Willer, and A. Schweiger, *J. Magn. Reson.* **130**, 86 (1998).
- [19] C.A. Reed and R.D. Bolskar, *Chem. Rev.* **100**, 1075 (2000).
- [20] P. Paul, K.-C. Kim, D. Sun, P.D.W. Boyd, and C.A. Reed, *J. Am. Chem. Soc.* **124**, 4394 (2002).
- [21] C. Coulon and R. Clérac, *Chem. Rev.* **104**, 5655 (2004).
- [22] C.A. Steren, H. van Willigen, and M. Fanciulli, *Chem. Phys. Lett.* **245**, 244 (1995).
- [23] T. Eickelkamp, S. Roth, and M. Mehring, *Mol. Phys.* **95**, 967 (1998).